

Electronic Supplementary Information (ESI) for Chemical Communications. This journal
is (c) The Royal Society of Chemistry 2023.
Electronic Supplementary Information (ESI)

A blade-like CoZn metal organic frameworks-based flexible quasi-solid Zn-ion battery

Yajun Zhu,^a Tianli Han,^a Xirong Lin,^b Huigang Zhang,^c Chaoquan Hu,^{*c} and Jinyun Liu^{*a}

Experimental details

Preparation of the Co-MOFs/CC: 1.6 mmol $\text{Co}(\text{NO}_3)_2 \cdot 6\text{H}_2\text{O}$ was added to 50 mL deionized water as solution A, and 20 mmol 2-methylimidazole was added to 50 mL deionized water as solution B. Subsequently, solution A was quickly transferred to solution B and stirred for 10 min. Then carbon cloth was added to the solution and soaked for 5 h. Finally, it was washed several times with water and ethanol and dried overnight at 60 °C.

Preparation of the CoZn-MOFs/CC: 1.6 mmol $\text{Co}(\text{NO}_3)_2 \cdot 6\text{H}_2\text{O}$ and 0.8 mmol $\text{Zn}(\text{NO}_3)_2 \cdot 6\text{H}_2\text{O}$ were dissolved in 50 mL deionized water as solution A; At the same time, 20 mmol 2-methylimidazole was added to 50 mL deionized water and dissolved as solution B. Then, the solution A was quickly transferred to the solution B and stirred for 10 min. Then carbon cloth was added to the solution and soaked for 5 h.

Preparation of self-healing hydrogel electrolyte: At 90 °C, appropriate amounts of manganese sulfate and zinc acetate were dissolved in 20 mL deionized water, and then 5 g

PVA was added. After stirring slowly for 2 h, the hydrogel was cooled in a petri dish and left overnight to obtain PAS hydrogel.

Characterization: SEM (Hitachi S-8100, 5 kV), TEM (Hitachi HT-7700), and XRD (Bruner D8 Advance) were used for morphology, structure and composition. XPS (ESCALAB 250) was used to analyze the different valence states. BET analyzer (ASAP 2460) was employed to measure the specific surface area and pore-size distribution. The hydrogels were treated with liquid nitrogen and placed in a freeze-dryer oven for 24 h. The functional groups of Co-MOFs and CoZn-MOFs were studied by FT-IR spectroscopy (IR-21IR-21) and Raman spectroscopy (Renishaw, in Via).

Battery construction and electrochemical tests: Zn-ion batteries prepared with PAS hydrogel electrolyte, CoZn-MOFs/CC cathode and Zn anode were assembled with a polyethylene film. The batteries were bent to 30°, 60°, 90°, 120°, 150° and 180°. In addition, for comparison, a conventional 2032-typed coin cell was assembled using the prepared cathode, Zn foil and glass fiber separator. and compared the electrochemical performance of the Co-MOFs pouch cell. The electrolyte was prepared by dissolving 1.5 M ZnSO₄ and 0.5 M MnSO₄. CV curves and electrochemical impedance spectroscopy (EIS) were tested on an electrochemical workstation (Chenhua, Chi-660E).

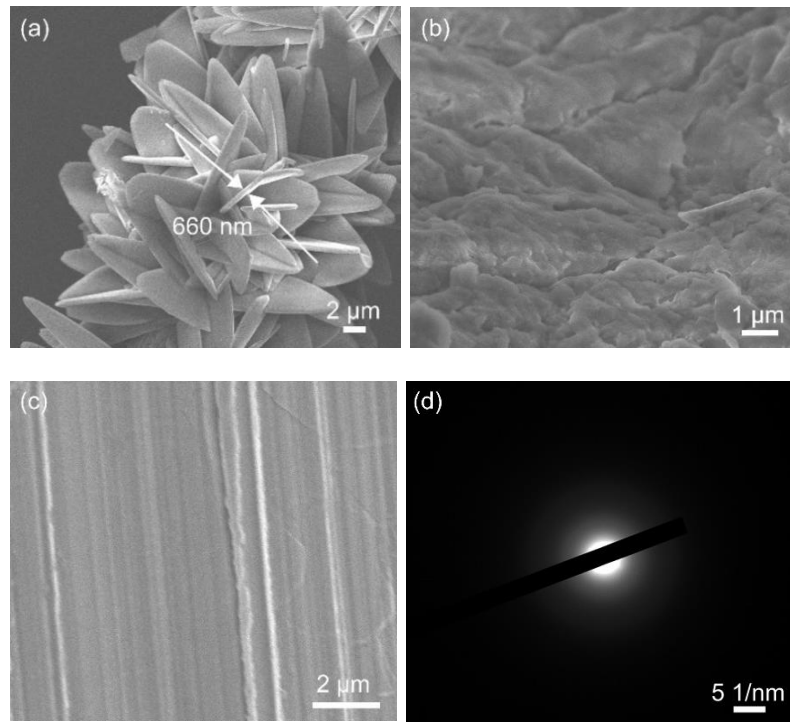


Fig. S1 SEM images of the (a) 3D CoZn-MOFs on carbon cloth, (b) hydrogel electrolyte, and (c) Zn anode before cycling. (d) SAED pattern of CoZn-MOFs.

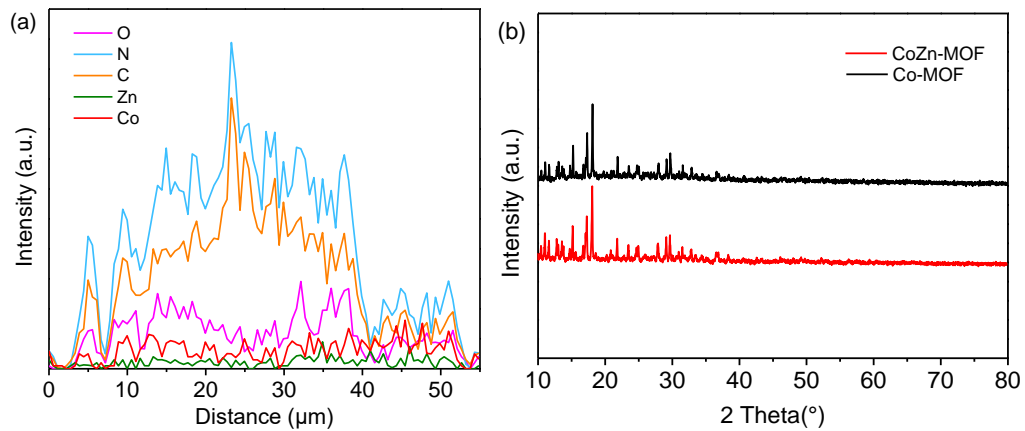


Fig. S2 (a) The line-scanning curves. (b) XRD patterns of Co-MOFs and CoZn-MOFs.

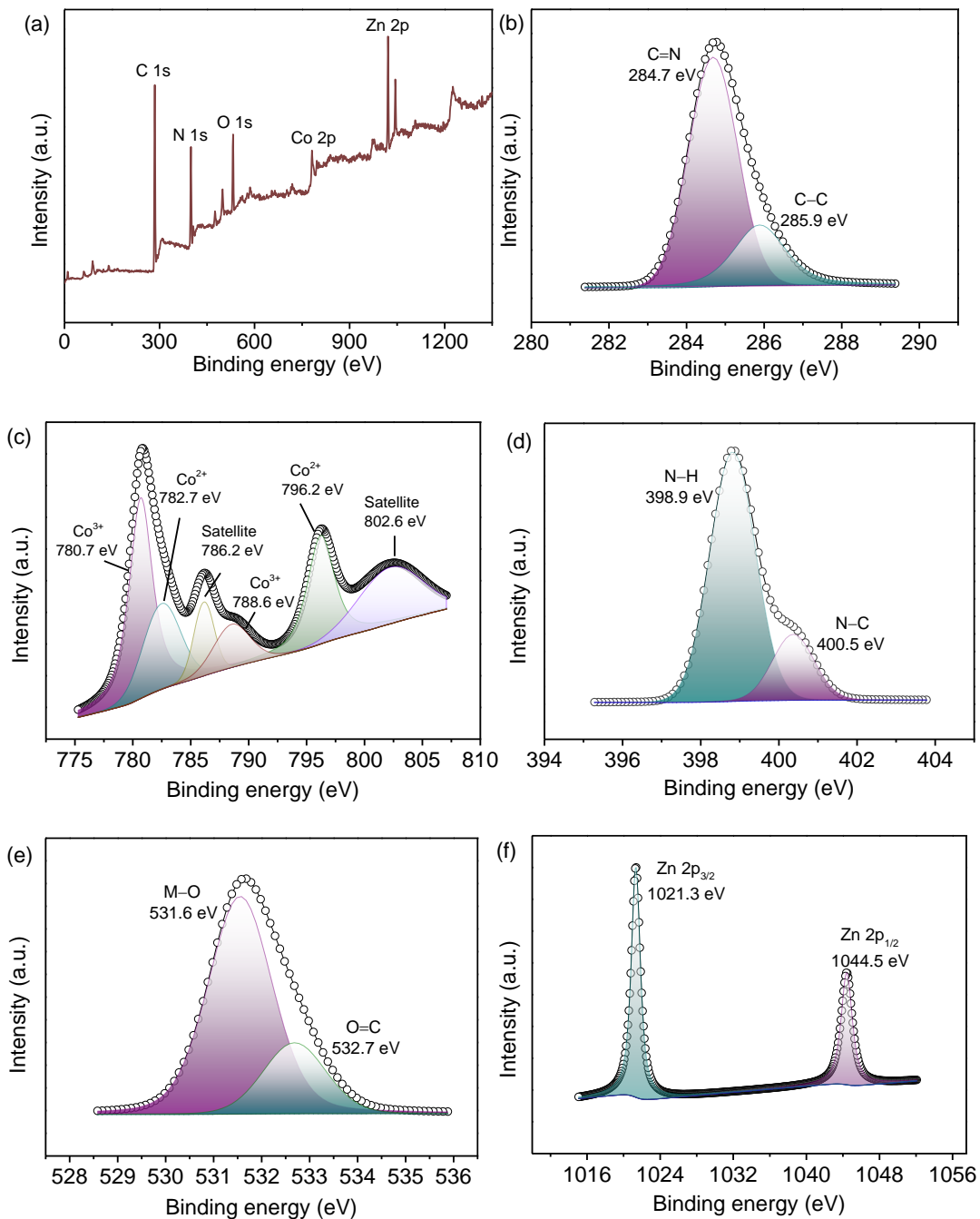


Fig. S3 XPS spectra of the CoZn-MOFs: (a) survey spectrum, (b-f) C 1s, Co 2p, N 1s, O 1s and Zn 2p.

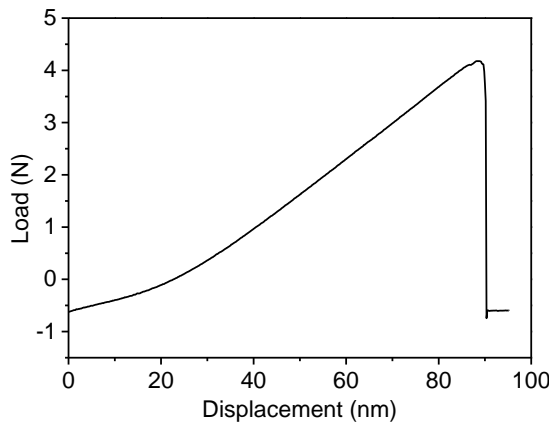


Fig. S4 The load-displacement curve of PAS hydrogel.

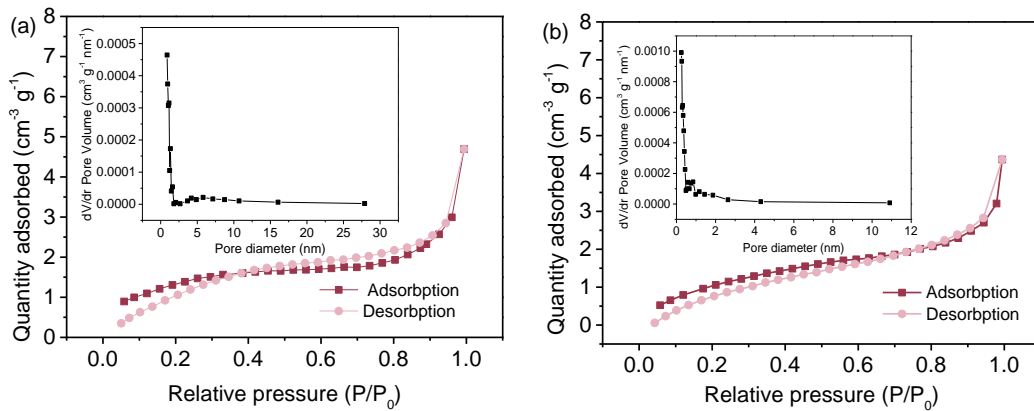


Fig. S5 (a,b) N₂ adsorption-desorption isotherm of Co-MOFs and CoZn-MOFs. Inset shows the pore-size distribution.

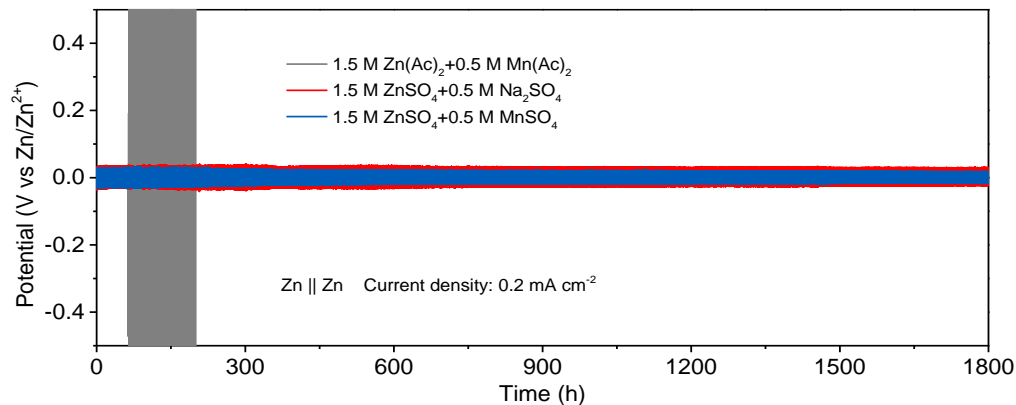


Fig. S6 Zn stripping/plating of Zn|Zn cell using different electrolytes at 0.2 mA cm⁻².

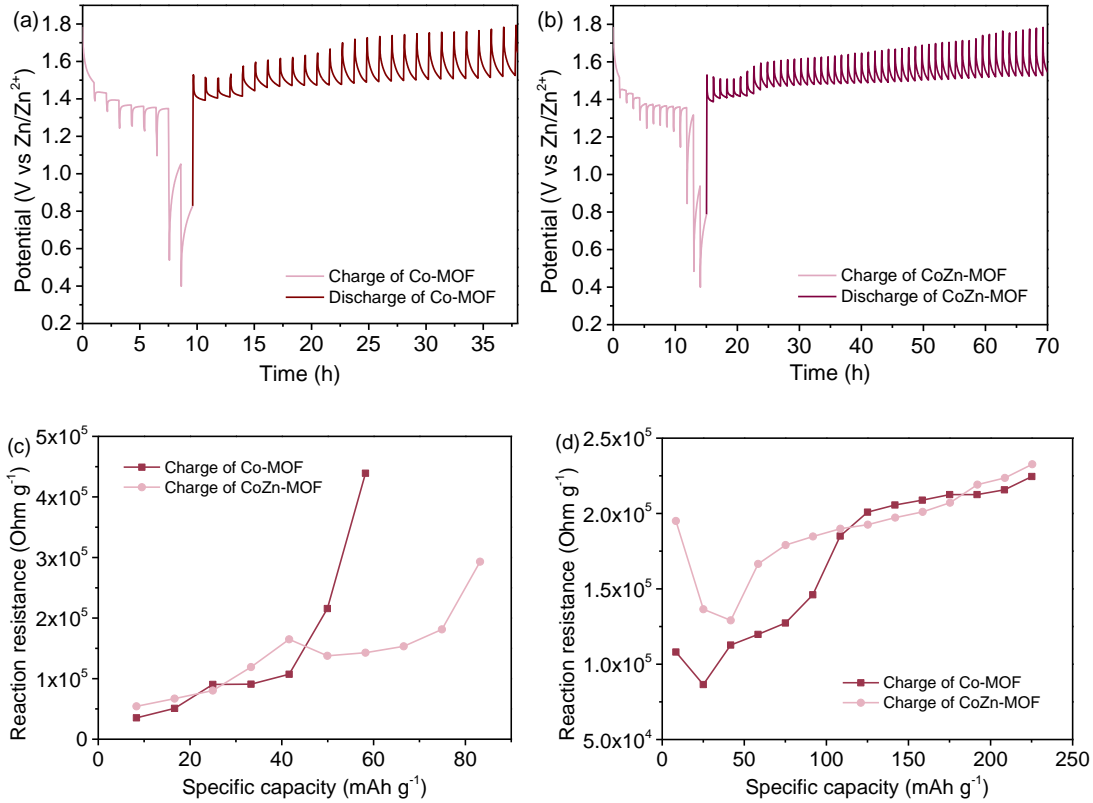


Fig. S7 GITT time-potential distribution of the battery based on (a) Co-MOFs and (b) CoZn-MOFs. *In-situ* reaction resistance of the battery based on Co-MOFs and CoZn-MOFs during (c) discharge and (d) charge.

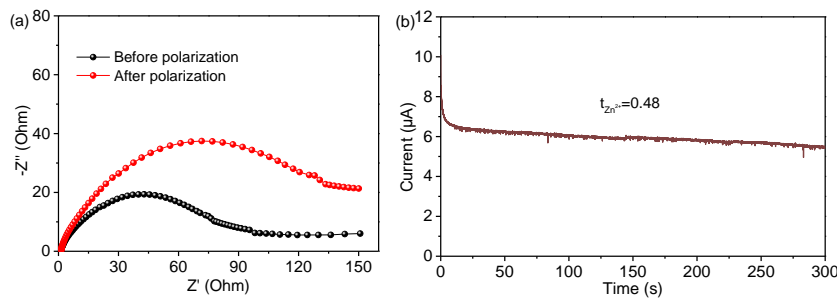


Fig. S8 (a) Impedance spectra of PAS before and after polarization. (b) The change of current with time during polarization when 1 mV voltage was applied at room temperature.

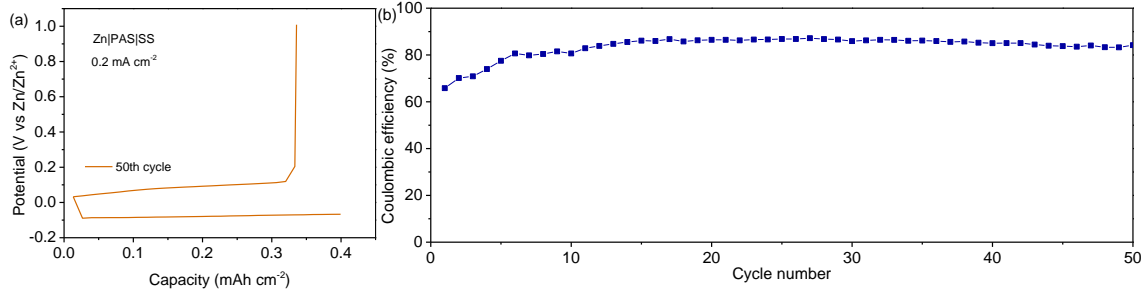


Fig. S9 (a) Charge-discharge curves and (b) Coulombic efficiency of Zn|PAS|SS asymmetry battery cycling at 0.2 mA cm^{-2} .

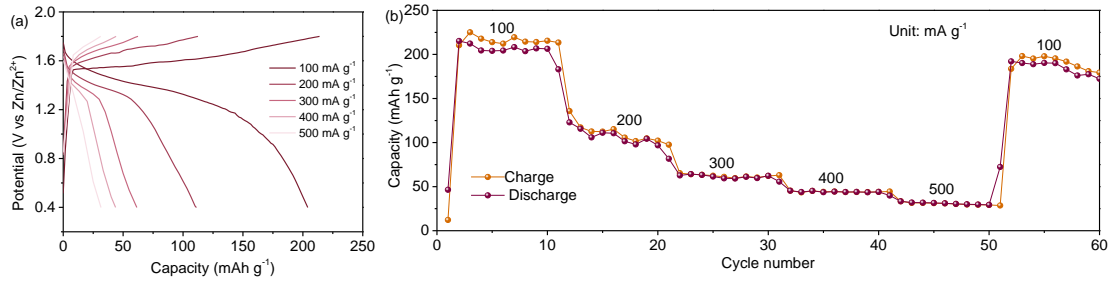


Fig. S10 (a) Discharge-charge profiles during rate-performance measurements. (b) Rate-performance of CoZn-MOFs with rates varying from 100 to 500 mA g^{-1} .

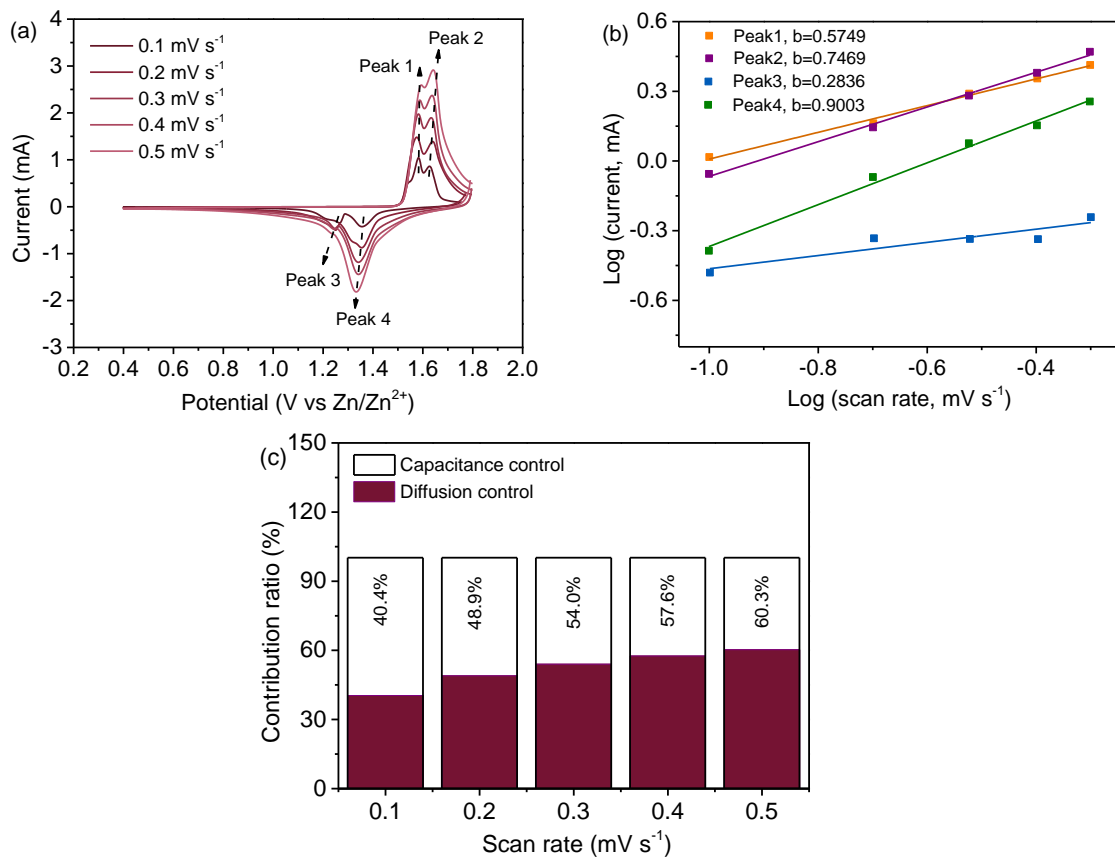


Fig. S11 (a) CV curves at 0.1 to 0.5 mV s⁻¹. (b) Fitted line plots of log(current) versus log(scan rate) for different redox peaks. (c) Ratio of capacitance to diffusion control contribution.

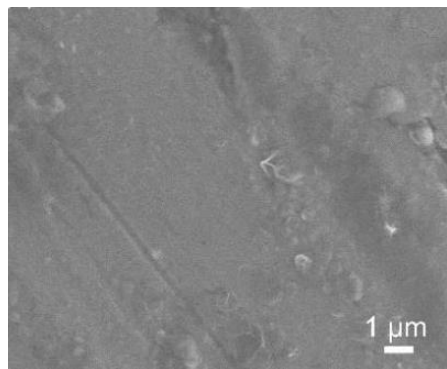


Fig. S12 SEM image of the Zn anode after 200 cycles.

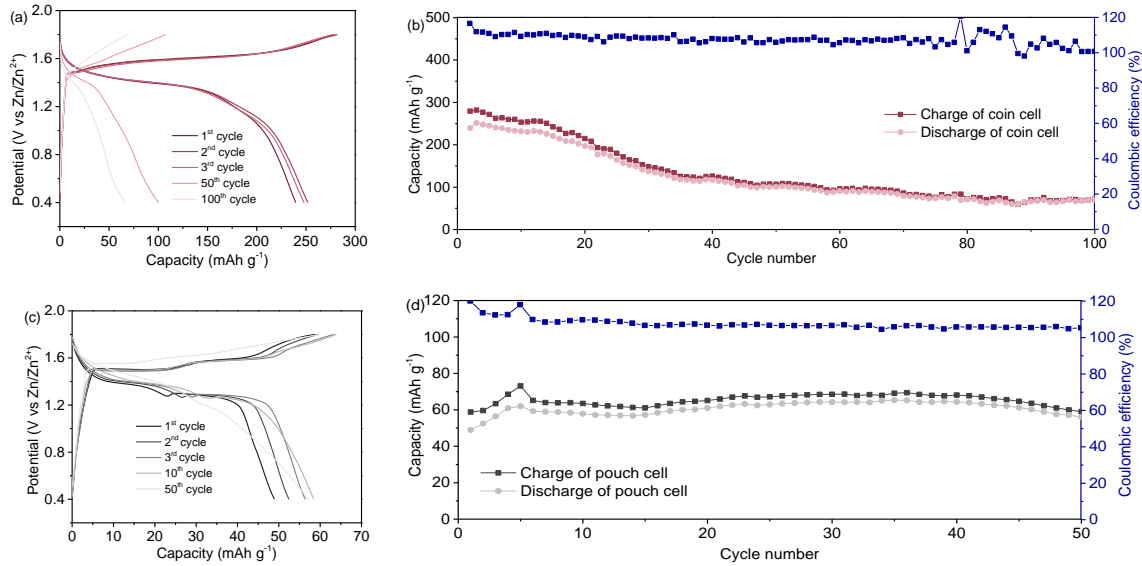


Fig. S13 (a) Galvanostatic charge-discharge curves and (b) cycling performance of the CoZn-MOFs based coin cell at 100 mA g⁻¹. (c) Charge-discharge curves and (d) cycling performance of the Co-MOFs pouch cell at 100 mA g⁻¹.

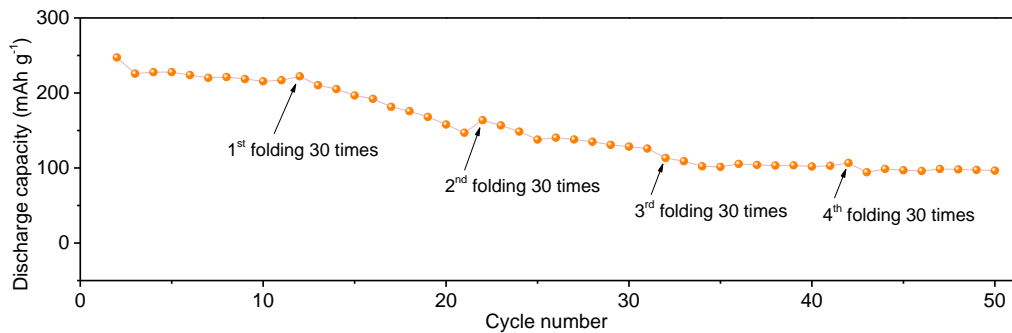


Fig. S14 Cycling performance at 100 mA g⁻¹ when the battery was repeatedly folded at 180° for 30 times.

Table S1. Comparison on the electrochemical performance of some Zn-ion batteries.

| Cathode | Electrolyte | Capacity /mAh g ⁻¹ | Rates /A g ⁻¹ | Cycle numbers | Ref. |
|---|---|-------------------------------|--------------------------|---------------|-----------|
| Ni-PTA | 3.0 M ZnSO ₄ + 0.2 M MnSO ₄ | 10 | 0.1 | 50 | 1 |
| KMn ₈ O ₁₆ | 1.0 M ZnSO ₄ + 0.05 M MnSO ₄ | 77 | 0.1 | 100 | 2 |
| Phenazine | 2.0 M ZnSO ₄ | 28 | 0.1 | 200 | 3 |
| α -MnO ₂ | 2.0 M ZnSO ₄ | 96.8 | 0.1 | 50 | 4 |
| ZnMnCoO ₄ | 2.0 M ZnSO ₄ + 0.1 M MnSO ₄ | 39 | 0.2 | 120 | 5 |
| Mn (BTC) | 2.0 M ZnSO ₄ + 0.1 M MnSO ₄ | 27 | 0.1 | 50 | 6 |
| Layered MnO ₂ | 1 M ZnSO ₄ | 97 | 0.1 | 50 | 7 |
| Prussian blue analogue | 1M choline acetate-water + zinc acetate | 54 | 0.1 | 50 | 8 |
| ZnMn ₂ O ₄ | 2.0 M ZnSO ₄ + 0.1 M MnSO ₄ | 67 | 0.1 | 40 | 9 |
| MnO ₂ | 1 M ZnSO ₄ + 0.05 M H ₂ SO ₄ | 89.5 | 0.3 | 55 | 10 |
| δ -MnO ₂ | 0.3 M ZnCl ₂ | 39 | 0.1 | 150 | 11 |
| Perylene-3,4,9,10-tetracarboxylic diimide | 3.0 M ZnSO ₄ | 73 | 0.1 | 200 | 12 |
| V ₂ O ₅ | Solid Zn-ion conductors | 58 | 0.02 | 300 | 13 |
| PANI/CNT | PVA-based gel electrolyte | 50 | 0.1 | 480 | 14 |
| MnO ₂ /CC | PAM/ZnSO ₄ -MnSO ₄ | 91.7 | 0.1 | 30 | 15 |
| CoZn-MOFs/CC | PAS hydrogel | 102 | 0.1 | 200 | This work |

References

- 1 C. Li, C. Zheng, H. Jiang, S. Bai, J. Jia, *J. Alloy. Compd.*, 2021, **882**, 160587.
- 2 J. Cai, X. Wu, S. Yang, C. Li, F. Tang, J. Chen, Y. Chen, Y. Xiang, X. Wu, Z. He, *Front. Chem.*, 2018, **6**, 352.
- 3 Q. Wang, Y. Liu, P. Chen, *J. Power Sources*, 2020, **468**, 228401.
- 4 X. Guo, J. Zhou, C. Bai, X. Li, G. Fang, S. Liang, *Mater. Today Energy*, 2020, **16**, 100396.
- 5 A. Baby, B. Senthilkumar, P. Barpanda, *ACS Appl. Energy Mater.*, 2019, **2**, 3211-3219.
- 6 X. Pu, B. Jiang, X. Wang, W. Liu, L. Dong, F. Kang, C. Xu, *Nano-Micro Lett.*, 2020, **12**, 152.
- 7 M. H. Alfaruqi, S. Islam, D. Y. Putro, V. Mathew, S. Kim, J. Jo, S. Kim, Y. K. Sun, K. Kim, J. Kim, *Electrochim. Acta*, 2018, **276**, 1-11.
- 8 Z. Liu, P. Bertram, F. Endres, *J. Solid State Electr.*, 2017, **21**, 2021-2027.
- 9 J. W. Lee, S. D. Seo, D. W. Kim, *J. Alloy. Compd.*, 2019, **800**, 478-482.
- 10 C. Wu, H. Tan, W. Huang, W. Li, K. N. Dinh, C. Yan, W. Wei, L. Chen, Q. Yan, *Adv. Funct. Mater.*, 2020, **30**, 2003187.
- 11 W. Kao-ian, R. Pornprasertsuk, P. Thamyongkit, T. Maiyalagan, S. Kheawhom, *J. Electrochem. Soc.*, 2019, **166**, 1063-1069.
- 12 N. Liu, X. Wu, Y. Zhang, Y. Yin, C. Sun, Y. Mao, L. Fan, N. Zhang, *Adv. Sci.*, 2020, **7**, 2000146.
- 13 J. Wang, Z. Zhao, G. Lu, Y. Zhang, Q. Kong, J. Zhao, G. Cui, *Mater. Today Energy*, 2021, **20**, 100630.
- 14 W. Du, J. Xiao, H. Geng, Y. Yang, Y. Zhang, E. H. Ang, M. Ye, C. Li, *J. Power Sources*, 2020, **450**, 227716.
- 15 F. Wu, X. Gao, X. Xu, Y. Jiang, X. Gao, R. Yin, W. Shi, W. Liu, G. Lu, X. Cao, *ChemSusChem*, 2020, **13**, 1537-1545.